

# Persistent changes in the dorsal root ganglion nociceptor translatoe governs hyperalgesic priming in mice: roles of GPR88 and Meteorin

Ishwarya Sankaranarayanan<sup>a</sup>, Moeno Kume<sup>a</sup>, Ayaan Mohammed<sup>a</sup>, Juliet M. Mwirigi<sup>a</sup>, Nikhil Nageswar Inturi<sup>a</sup>, Gordon Munro<sup>b</sup>, Kenneth A. Petersen<sup>b</sup>, Diana Tavares-Ferreira<sup>a</sup>, Theodore J. Price<sup>a,\*</sup>

## Abstract

Hyperalgesic priming is a model system that has been widely used to understand plasticity in painful stimulus-detecting sensory neurons, called nociceptors. A key feature of this model system is that following priming, stimuli that do not normally cause hyperalgesia now readily provoke this state. We hypothesized that hyperalgesic priming occurs because of reorganization of translation of mRNA in nociceptors. To test this hypothesis, we used paclitaxel treatment as the priming stimulus and translating ribosome affinity purification to measure persistent changes in mRNA translation in Na<sub>v</sub>1.8+ nociceptors. Translating ribosome affinity purification sequencing revealed 161 genes with persistently altered mRNA translation in the primed state. Among these genes, we identified *Gpr88* as upregulated and *Metrn* as downregulated. To provide functional evidence for these changes in hyperalgesic priming in a related priming model, we used the interleukin-6 priming model. A GPR88 agonist injection into the paw had no effect in naive mice but caused mechanical hypersensitivity and grimacing responses in female primed mice. Systemic Meteorin treatment in primed mice completely reversed established hyperalgesic priming mechanical hypersensitivity and grimacing responses to prostaglandin E<sub>2</sub> in female mice. Our work demonstrates that altered nociceptor translatoes are causative in producing hyperalgesic priming in multiple models in female mice.

**Keywords:** Chemotherapy-induced peripheral neuropathy, Hyperalgesic priming, Translating ribosome affinity purification, GPR88, Meteorin, IL6-mediated hyperalgesic priming

## 1. Introduction

Injuries like surgical wounds, inflammatory mediators such as cytokines, and agents that can cause neuropathies, such as paclitaxel, provoke mechanical hyperalgesia and signs of ongoing pain in rodents and in humans. These pain-causing insults also produce a state referred to as hyperalgesic priming, wherein animals display a painful response to a dose of a stimulus, like prostaglandin E<sub>2</sub> (PGE<sub>2</sub>), that does not normally cause pain in unprimed rodents.<sup>48,49</sup> The existence of this primed state, which can last from weeks to months after the initial insult, indicates that memory-like changes in the peripheral and/or central nervous system occur that maintain this primed state.<sup>45,48,49</sup> Inhibitors of transcription and mRNA translation applied to the peripheral terminals and to the cell bodies of dorsal root ganglion (DRG)

nociceptors can prevent the development of hyperalgesic priming, and inhibitors of mRNA translation can reverse an established primed state.<sup>3,6,11–15,26,27,36,40,41</sup> These findings suggest that the mRNA translational state of nociceptors is reorganized by the initial insult that causes the primed state and that this change continues even after the resolution of the initial pain state. However, this idea has not been formally tested.

We tested the hypothesis that hyperalgesic priming in mice is accompanied by a persistent change in the repertoire of translated mRNAs in nociceptors when mice are primed but showing no overt signs of mechanical hypersensitivity or ongoing pain. To do this, we used the translating ribosome affinity purification (TRAP) technique.<sup>19,20</sup> This technology uses a Cre-driven expression of the ribosomal L10a protein fused to an enhanced green fluorescent protein (eGFP) to enable pull-down of translating ribosomes, coupled with RNA sequencing to assess the active translatoe of a specific cell type.<sup>19,20</sup> We used the *Scn10a* gene as a Cre-driver because this gene is exclusively expressed in sensory neurons of mice and is greatly enriched in nociceptors vs other cell types.<sup>54</sup> We have previously used this technique to gain insight into sex differences in translation in the DRG,<sup>56</sup> difference in translatoes between the DRG and trigeminal ganglion,<sup>34</sup> and to understand translational reorganization in nociceptors caused by the chemotherapeutic paclitaxel, but at the peak of paclitaxel-induced pain behaviors.<sup>33</sup> Our findings support the hypothesis that translational reorganization in nociceptors is linked to the persistence of hyperalgesic priming. Moreover, we identified targets amongst translationally upregulated and downregulated mRNAs that can be activated to reveal the expression of the primed state or can be

Sponsorships or competing interests that may be relevant to content are disclosed at the end of this article.

<sup>a</sup> Department of Neuroscience, Center for Advanced Pain Studies, School of Behavioral and Brain Sciences, University of Texas at Dallas, Richardson, TX, <sup>b</sup> Hoba Therapeutics ApS, Copenhagen, Denmark

\*Corresponding author. Address: Department of Neuroscience, The University of Texas at Dallas, 800 W Campbell Dr, BSB 14.102, Richardson, TX 75080, United States. Tel.: 972-883-4311. E-mail address: Theodore.price@utdallas.edu (T.J. Price).

Supplemental digital content is available for this article. Direct URL citations appear in the printed text and are provided in the HTML and PDF versions of this article on the journal's Web site ([www.painjournalonline.com](http://www.painjournalonline.com)).

© 2025 International Association for the Study of Pain  
<http://dx.doi.org/10.1097/j.pain.0000000000003523>

increased to resolve the primed state, respectively. This work adds to a growing body of evidence that nociceptor plasticity is entrenched by multiple levels of gene expression regulation and requires active intervention to achieve resolution.<sup>10,16,22,24,29,32,44</sup>

## 2. Materials and methods

### 2.1. Animals

Rosa26<sup>fsTRAP</sup> mice were crossed with Na<sub>v</sub>1.8<sup>cre</sup> mice on a C57BL/6J genetic background to generate Na<sub>v</sub>1.8-TRAP mice, which express a fused eGFP-L10a protein in Na<sub>v</sub>1.8-positive neurons.<sup>19,34,54,56</sup> Translating ribosome affinity purification experiments were conducted on female Na<sub>v</sub>1.8-TRAP littermates, whereas behavioral experiments were performed on both C57BL/6J mice and Na<sub>v</sub>1.8-TRAP mice that were 8 to 10 weeks old. The mice were group housed with a maximum of 4 per cage and had food and water available ad libitum. They were maintained on a 12-hour light–dark cycle at a room temperature of 21 ± 2°C. All procedures were approved by the Institutional Animal Care and Use Committee at the University of Texas at Dallas.

### 2.2. Injections

Paclitaxel (Y0000698; Sigma-Aldrich, St. Louis, MO) was dissolved in a 1:1 solvent mixture of Kolliphor EL (Sigma-Aldrich) and ethanol, as previously described.<sup>51,52</sup> Female Na<sub>v</sub>1.8-TRAP mice were administered paclitaxel diluted in sterile Dulbecco phosphate-buffered saline (Thermo Scientific, Waltham, MA) or vehicle solvent intraperitoneally at a dosage of 4 mg/kg every other day, resulting in a cumulative dosage of 16 mg/kg. C57BL/6J mice were administered intraplantar injections of recombinant human interleukin 6 (IL-6) (206-IL; R&D Systems, Minneapolis, MN) at a dosage of 0.1 ng or 100 ng PGE<sub>2</sub> (cat# 14010; Cayman Chemical, Ann Arbor, MI) dissolved in sterile saline for priming experiments. RTI-13951-33 hydrochloride (MedChem Express, Monmouth Junction, NJ), a GPR88 agonist, was dissolved in dimethyl sulfoxide (DMSO) at a stock concentration of 5 mM and then diluted in sterile saline and administered through intraplantar injection at doses of either 100 ng or 1 µg into the hind paw. Recombinant mouse Meteorin (rmMeteorin; R&D Systems, #3475) or vehicle control (Dulbecco phosphate-buffered saline) was administered once subcutaneously at 1.8 mg/kg using a 30-gauge needle. The investigator was blinded to the treatment during all injections.

### 2.3. Behavioral testing

Mice were habituated for 1 hour before testing for mechanical sensitivity in a clear acrylic behavioral chamber. Mechanical paw withdrawal thresholds were assessed using the Dixon up–down method with calibrated von Frey filaments (Stoelting, Dale, IL), ranging from 0.16 to 2 g, applied perpendicular to the midplantar surface of the hind paw.<sup>7</sup> A positive response was defined as an immediate flicking or licking behavior upon application of the filament. The investigator was blinded to treatment conditions during all days of testing.

The Mouse Grimace Scale was used to assess spontaneous pain-like behaviors in mice, as described by Langford et al.<sup>28</sup> Mice were scored in 5 facial categories: orbital tightening, nose bulge, cheek bulge, ear position, and whisker position. Each category was rated on a scale from 0 (not present), 1 (moderately present) to 2 (severely present), and the average score was used

to represent the overall level of facial changes. Mice were placed in an acrylic observation chamber, providing a clear view of the face for the observer. The investigator was blinded to the treatment conditions during the assessment. Grimace scores were assessed before testing for mechanical sensitivity to ensure that grimacing responses were not a result of mechanical stimulation with von Frey filaments.

### 2.4. Translating ribosome affinity purification

Translating ribosome affinity purification was done as previously described by Tavares-Ferreira et al.<sup>56</sup> Na<sub>v</sub>1.8-TRAP female mice (4 mice per condition) were euthanized by cervical dislocation and decapitation under isoflurane anesthesia, and their DRGs were rapidly dissected in ice-cold dissection buffer (1 × hanks buffered salt solution (HBSS) [14065006; Invitrogen, Waltham, MA], 2.5 mM HEPES-NaOH [pH 7.4], 35 mM glucose, 5 mM MgCl<sub>2</sub>, 100 µg/mL cycloheximide, 0.2 mg/mL emetine). The DRGs were then transferred to ice-cold Precellys tissue homogenizing CKMix tubes containing lysis buffer (20 mM HEPES, 12 mM MgCl<sub>2</sub>, 150 mM KCl, 0.5 mM dithiothreitol [DTT]), 100 µg/mL cycloheximide, 20 µg/mL emetine, and 80 U/mL SUPERase-IN (Promega, Madison, WI). Samples were homogenized using a Precellys MiniLys Tissue Homogenizer at 10-second intervals for a total of 80 seconds in a cold room (4°C). The lysate was then centrifuged at ×2000g for 5 minutes to obtain the post nuclear fraction. Following this, 1% NP-40 and 30 mM 1,2-dihexanoyl-sn-glycero-3-phosphocholine were added, and the samples were centrifuged at ×15,000g for 10 minutes to produce the postmitochondrial fraction. A 200-µL sample of this fraction was set aside for INPUT (bulk RNA-sequencing), whereas the remaining lysate was incubated with protein G-coated Dynabeads (Invitrogen) bound to 50-µg anti-GFP antibodies (HtzGFP-19F7 and HtzGFP-19C8; Memorial Sloan Kettering Centre, New York City, NY) for 3 hours at 4°C with end-over-end mixing. The beads were washed with high salt buffer (20 mM HEPES, 5 mM MgCl<sub>2</sub>, 350 mM KCl, 1% NP-40, 0.5 mM dithiothreitol, and 100 µg/mL cycloheximide), and RNA was extracted using the Direct-zol kit (Zymo Research, Irvine, CA) following the manufacturer's instructions. RNA yield was quantified using a Qubit (Invitrogen), and RNA quality was assessed using a Fragment Analyzer (Advanced Analytical Technologies, Heidelberg, Germany).

Libraries were prepared according to the manufacturer's instructions using the Total RNA Gold library preparation kit (with ribosomal RNA depletion) and sequenced on the NextSeq 2000 platform with 75-bp single-end reads. The sequencing was performed at the Genome Center, part of the University of Texas at Dallas Research Core Facilities.

### 2.5. Data analysis

RNA-seq read files (fastq files) were processed and analyzed following the methodology described by Tavares-Ferreira et al.<sup>56</sup> Quality assessment was conducted using FastQC (Babraham Bioinformatics, Cambridge, United Kingdom). Reads were trimmed based on Phred scores and per-base sequence content. The trimmed reads were then aligned to the reference genome and transcriptome (Gencode vM16 and GRCm38.p5) using STAR v2.2.1. Relative abundances in transcripts per million (TPM) for each gene in every sample were quantified using StringTie v1.3.5. Noncoding and mitochondrial genes were excluded from the analysis, and the TPMs for nonmitochondrial coding genes were renormalized to sum to 1 million.

We selected 14,955 genes above the 30th percentile in each INPUT sample, ensuring consistent detection of the transcriptome. Following this, we performed quantile normalization (qn) on all coding genes. For the IP samples, we calculated percentile ranks for the TPMs of these genes in each IP sample, focusing on genes above the 30th percentile from the INPUT samples. From this set, 12,944 genes were identified as consistently detected in the translome (IP samples), based on their expression at or above the 15th percentile in each sample and were quantile normalized. Differential gene expression analysis was performed by calculating the log<sub>2</sub>-fold change (based on median TPM values), strictly standardized mean difference (SSMD), and the Bhattacharyya coefficient. This modified coefficient ranges from 0, indicating completely identical distributions, to +1 or -1, indicating entirely nonoverlapping distributions, with the sign determined by the log-fold change value. TPMs for all genes are shown in Supplementary File 1 (<http://links.lww.com/PAIN/C210>).

## 2.6. Statistics

Statistical analyses for behavioral data were conducted using GraphPad Prism 10. Data visualization was performed in Python (version 3.7; Anaconda distribution, Austin, TX). Results are presented as mean  $\pm$  SEM and were analyzed using 1-way or 2-way analysis of variance followed by post hoc tests for between-group comparisons. Effect sizes were determined by subtracting behavior scores for each time point from baseline measures. Absolute values were summed up and plotted for each group. All data are represented as mean  $\pm$  SEM with  $P < 0.05$  considered significant. Detailed statistical outcomes are provided in the figure legends. Bioinformatics analysis and data visualization coding was done in Python (version 3.7; Anaconda distribution). Schematic illustrations were created with BioRender (BioRender.com).

## 3. Results

Our previous work demonstrated changes in nociceptor translomes associated with paclitaxel neuropathy at the peak time point for mechanical hypersensitivity.<sup>33</sup> We have also shown that after the resolution of paclitaxel-induced pain behaviors, mice demonstrate hyperalgesic priming,<sup>21</sup> suggesting a persistent change in nociceptors that maintains this primed state.<sup>45,48,49</sup> Although there are many types of stimuli that can be used to induce hyperalgesic priming, the paclitaxel model is ideal for assessing the translome of nociceptors because it is a systemic treatment that affects all DRGs, which need to be pooled to obtain enough material for TRAP-seq experiments.<sup>33,56</sup> To explore nociceptor-specific changes in mRNA translation after overt pain behaviors induced by paclitaxel have resolved, but when mice are still primed, we used paclitaxel-treated female Na<sub>v</sub>1.8-TRAP mice (Fig. 1A). Behavioral testing revealed significant mechanical hypersensitivity in paclitaxel-treated mice compared with vehicle controls, which persisted for nearly 50 days before returning to baseline (Fig. 1B). Dorsal root ganglia were dissected from paclitaxel- and vehicle-treated animals at day 59, followed by immunoprecipitation of translating ribosomes from DRG neurons, mRNA purification, and RNA-seq. We acquired both the input sample (IN sample), which corresponds to the total mRNA present in the DRG, and the IP sample, which corresponds with the mRNA bound to eGFP-tagged ribosomes that are actively being translated (Fig. 1C).

We conducted hierarchical clustering and heatmap analysis using the correlation coefficients of coding gene TPMs. This analysis revealed that the IN and IP samples were segregated into 2 distinct molecular profiles, demonstrating a clear separation between the actively translated mRNAs captured by TRAP-seq and the bulk RNA population analyzed by RNA-seq (Fig. 2A). We also identified a clear separation of each biological replicate between the TRAP-seq and bulk RNA-seq from the heatmap analysis (Fig. 2B). We identified high correlation coefficients across gene TPMs between input and IP samples (shown), revealing strong reproducibility across experiments (Fig. 2C). Percentile ranks were calculated for gene expression levels for each RNA-seq and TRAP-seq sample. Using these order statistics, we identified 14955 genes ( $\geq$ 30th percentile) that were consistently detected in at least one of the RNA-seq samples, and for the TRAP-seq samples, we detected 12944 genes ( $\geq$ 15th percentile). These findings align with previous mouse DRG RNA-seq and TRAP-seq studies.<sup>33,34,56</sup> We plotted the empirical probability densities of coding gene TPMs and observed a bimodal distribution, distinguishing genes that are consistently detected from those that are lowly expressed. To account for differences in sequencing depth and ensure sample comparability, we applied quantile normalization to the TPM expression levels, represented as qnTPMs (Fig. 2D). To verify the specificity of TRAP-seq for purifying translating mRNAs from nociceptors, we examined sets of control genes known to be enriched in either neuronal or nonneuronal cells within the DRG. Nociceptor mRNAs, such as *Calca*, *Trpv1*, *Scn10a*, and *Prph*, exhibited higher relative abundance in the IP sample. Conversely, nonneuronal genes, including glial markers like *Mpz*, *Mbp*, and *Gfap*, were found to be de-enriched in the IP samples (Fig. 2E). We identified differentially expressed (DE) genes by calculating the log<sub>2</sub>-fold change across the samples. Additionally, we employed 2 other statistics: the SSMD<sup>62,63</sup> of TPM percentile ranks and the Bhattacharyya coefficient of qnTPMs. These measures quantified the effect size and controlled for within-group variability. For a gene to be considered DE, we applied stringent criteria:  $|\log_2 - \text{fold change}| > 0.58$  (equivalent to a fold change  $> 1.5$ ),  $|\text{SSMD}| > 0.97$ , and Bhattacharyya coefficient  $< 0.5$ . We then plotted the SSMD values against the log<sub>2</sub>-transformed fold change for autosomal genes in IP samples (Fig. 2F).

We identified 122 DE genes in the IN samples, with *Dusp14*, *Eef2kmt*, and *Mrgprx1* upregulated and *Mrgprh* downregulated. In the mRNAs associated with translating ribosomes (IP samples), we found a total of 160 DE genes, with 79 upregulated and 81 downregulated (Supplementary File 2, <http://links.lww.com/PAIN/C210>). We observed only 4 genes that overlapped between the IP and IN samples with genes, such as *Mok*, *Tmem254a*, *Tmem254b*, and *Nup37*. Additionally, we found that the genes *Mok*, *Prcc*, *Iltk*, *Fhdcl*, *Cars*, and *Ctu2* overlapped between our previous study doing TRAP sequencing at the peak of paclitaxel-evoked pain and the resolution of paclitaxel-induced pain.<sup>33</sup> *Mok* is part of the MAP kinase pathway, suggesting continued involvement of this posttranslational pathway from the early pain state to the time point of the primed state. Among the upregulated genes in the IP samples, several were already implicated in the sensitization of nociceptors, such as the prostaglandin E receptor 1 and transforming growth factor beta1<sup>30,39,53,55,64</sup> (Fig. 3A). Conversely, the downregulated genes included several involved in neuronal function, such as sodium voltage-gated channel alpha subunit 3 (*Scn3a*) and solute carrier family 1 member 2 (*Slc1a2*) (Fig. 3B).



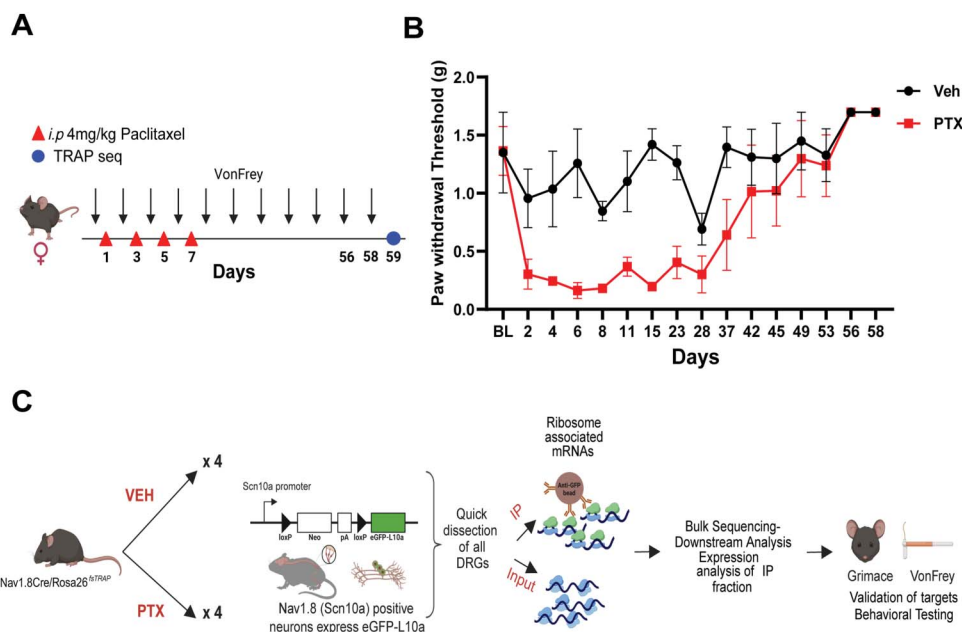


**Figure 1.** Cell type-specific gene expression during the resolution phase of paclitaxel-induced mechanical hypersensitivity. (A) Schematic representation of the dosing paradigm for paclitaxel treatment and behavioral testing using von Frey filaments. (B) Paw withdrawal thresholds were reduced with the administration of paclitaxel in a cohort of female *Nav1.8cre/Rosa26<sup>fTRAP</sup>* mice. (C) Outline of the workflow for translating ribosome affinity purification (TRAP) sequencing. *Nav1.8cre/Rosa26<sup>fTRAP</sup>* mice were administered vehicle or paclitaxel, and we euthanized on day 59 day upon returning to baseline mechanical thresholds. Whole dorsal root ganglia (DRGs) were dissected and homogenized, and total RNA (INPUT) was extracted from the lysate. mRNAs bound to ribosomes (IP) were further isolated using eGFP-coated beads. Samples were sequenced and potential genes were validated using behavioral testing. eGFP, enhanced green fluorescent protein.

We then focused on the most highly upregulated DE gene in the IP sample, *Gpr88* (Fig. 4A), a gene encoding a G protein-coupled receptor (GPCR) with no known endogenous ligand that is highly expressed in the striatum and cortex, associated with neurological disorders, and has several recently described synthetic agonists.<sup>60</sup> We investigated whether a GPR88 agonist could be used in a similar manner to PGE2 to reveal the expression of the primed state by inducing mechanical hypersensitivity and grimacing only in primed animals. To reduce the time needed to assess the role of GPR88 in hyperalgesic priming and to test the generalizability of the target in other priming models, we used IL-6 as the priming stimulus. Interleukin 6 is a well-studied proinflammatory mediator known to sensitize neurons in the DRG and produce an initial pain state that lasts for only about 5 days.<sup>2,9,35,43</sup> We administered IL-6 into the paw and performed von Frey testing until the animals returned to baseline. Once the animals were back to baseline, they were injected with either a GPR88 agonist, RTI-13951-33 hydrochloride (100 ng or 1  $\mu$ g), or 100 ng PGE2 (Fig. 4B). Intraplantar administration of IL-6 to female mice produced mechanical hypersensitivity, which returned to baseline within a week post administration. Mice previously treated with IL-6 and primed showed mechanical hypersensitivity when given an intraplantar injection of RTI-13951-33, but mice previously treated with vehicle and not primed did not respond to even the 1- $\mu$ g dose of RTI-13951-33 (Fig. 4C). Primed mice also responded to the positive control 100-ng PGE2. Effect size calculation showed that only mice primed with IL-6 responded to either RTI-13951-33 or PGE2 (Fig. 4D). We also investigated grimacing behavior in these animals and observed that primed animals injected with either dose of the GPR88 agonist exhibited grimacing behaviors comparable to animals treated with IL-6 and PGE2 (Fig. 4E). This finding demonstrates that increased nociceptor translation of *Gpr88* is

linked to a behavioral response to a GPR88 agonist only observed in primed mice.

We identified the *Metrn* gene, which encodes Meteorin, a secreted protein with no known receptor originally reported to be expressed in neural progenitors and in astrocytes including radial glia,<sup>42</sup> as one of the downregulated genes in the IP sample (Fig. 5A). Previous studies have demonstrated an antinociceptive effect of Meteorin in neuropathic pain models in mice and rats,<sup>23,51,59</sup> but it has never been assessed in hyperalgesic priming models. We used the IL-6 priming model to assess whether recombinant mouse Meteorin (rmMTRN) treatment could block the expression of hyperalgesic priming revealed by PGE2 injection. Once animals returned to baseline mechanical thresholds after IL-6 administration, a single subcutaneous injection of rmMTRN (1.8 mg/kg) was administered 1 hour before the intraplantar PGE2 injection (Fig. 5B). Treatment with rmMTRN led to significant alleviation of mechanical hypersensitivity caused by PGE2 treatment (Figs. 5C and D). rmMTRN treatment also alleviated PGE2-induced grimacing behavior (Fig. 5E).

#### 4. Discussion

The most important finding emerging from this work is that even after the resolution of overt pain-related behaviors caused by a treatment that causes neuropathic pain in mice and humans, changes in nociceptor gene expression at the level of mRNA translation persist. This finding suggests that these neurons do not readily return to their baseline state and that this altered translational landscape is linked to pain susceptibility where a normally innocuous stimulus can now precipitate a return of the pain state. We provide evidence in support of this hypothesis with GPR88, the most translationally upregulated mRNA in the DRG of primed mice, and with Meteorin, which was translationally downregulated. Using the IL-6 priming

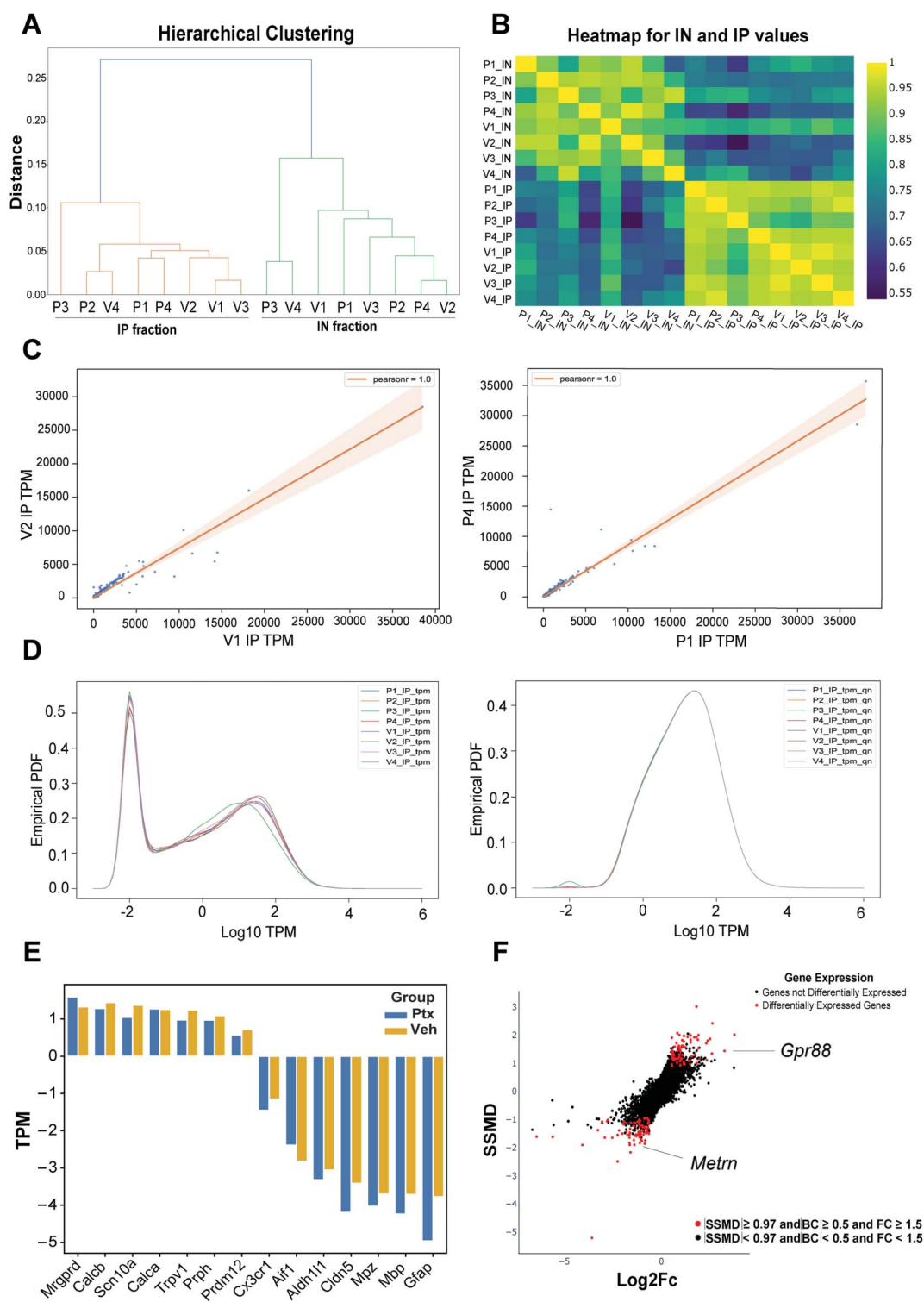


**Figure 2.** Nociceptor-specific translating ribosome affinity purification (TRAP) sequencing after resolution of paclitaxel-induced mechanical hypersensitivity: (A) Hierarchical clustering using the correlation coefficients showing separation between the IN and the IP samples. (B) Heatmap plot revealing a clear distinction between the biological replicates between the TRAP-seq and the INPUT samples. (C) Linear correlation plots show a higher correlation between the IP samples. (D) Empirical probability distribution of all coding genes using the raw TPMs and quantile normalized TPMs of all IP samples. (E) Higher expression is observed of neuronal genes (*Mrgprd*, *Calcb*, *Scn10a*, *Calca*, *Trpv1*, *Prph*) compared with nonneuronal genes (*Prdm12*, *Cx3cr1*, *Aif1*, *Mpz*, *Mbp*, *Gfap*) showing neuron-specific enrichment using TRAP. (F) Differentially translated mRNAs in the IP sample are shown by a dual-lightened plot against strictly standardized mean difference (SSMD) and log<sub>2</sub>-fold change.

model, we demonstrate that the increased translation of GPR88 causes IL-6-treated mice to become primed to a specific GPR88 agonist that is nonnoxious in vehicle-treated mice. Conversely, enhancing Meteorin signaling with

rmMTRN treatment reversed hyperalgesic priming. Collectively, our experiments demonstrate that persistent changes in nociceptor translation are a likely causative factor in the transition to a chronic pain state.

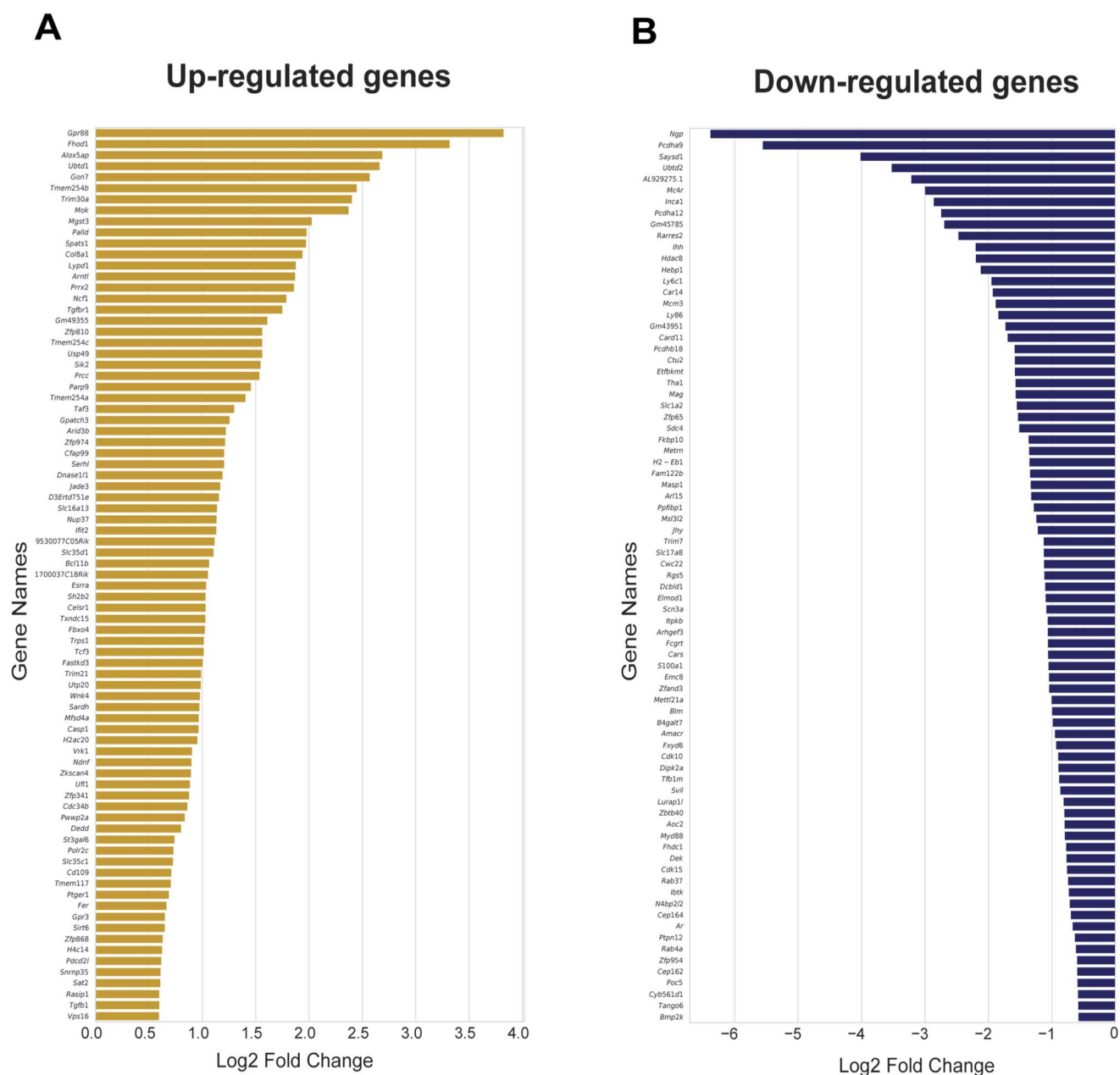


**Figure 3.** Differentially translated nociceptor-specific mRNAs after paclitaxel treatment. (A) Bar plot showing a log<sub>2</sub>-fold change of all upregulated differentially translated mRNAs in the IP sample. (B) Bar plot showing log<sub>2</sub>-fold change of all downregulated genes in the IP samples.

Translation regulation in nociceptors has long been recognized as a key mechanism that controls hyperalgesic priming.<sup>4,6,11–15,26,36,40,41,45</sup> At least 3 translation regulation mechanisms have been proposed to control translation in nociceptors in priming models: MNK-eIF4E signaling,<sup>8,27,33,40</sup> the mechanistic target of rapamycin kinase signaling,<sup>21,45</sup> and translation regulation at the 3' end of mRNAs through binding factors at the poly-A tail of mRNAs.<sup>4,6,13</sup> Although our study reveals mRNAs with altered translation in nociceptors in the primed state, we have not determined which of these pathways regulate the translation of specific subsets of mRNAs. Because these pathways may act in concert to control translation in sensitized nociceptors,<sup>33</sup> it is also possible that interfering with these pathways individually would have similar consequences. We observed shifts in translation efficiency for roughly equal upregulated and downregulated mRNAs. This observation is

consistent with MNK-eIF4E signaling, which does not appear to decrease overall translation in mouse or human neurons but instead shifts subsets of mRNAs to increased translation efficiency and others to decreased efficiency,<sup>1,17,35,37</sup> as we observed in our study. Because MNK-eIF4E signaling is engaged in nociceptors by paclitaxel treatment in mice<sup>33</sup> and by IL-6 in nociceptors in both mice<sup>35,40</sup> and humans,<sup>37</sup> we propose that MNK-eIF4E signaling is the most parsimonious signaling mechanism explaining the observations we have observed in the studies conducted here. This hypothesis can be tested in future experiments.

GPR88 is an orphan GPCR that does not have a known endogenous ligand or function, but several synthetic agonists have recently been described.<sup>60</sup> The receptor has garnered interest in the neuropsychopharmacology area due to phenotypes of the *Gpr88*-knockout mouse and genetic association

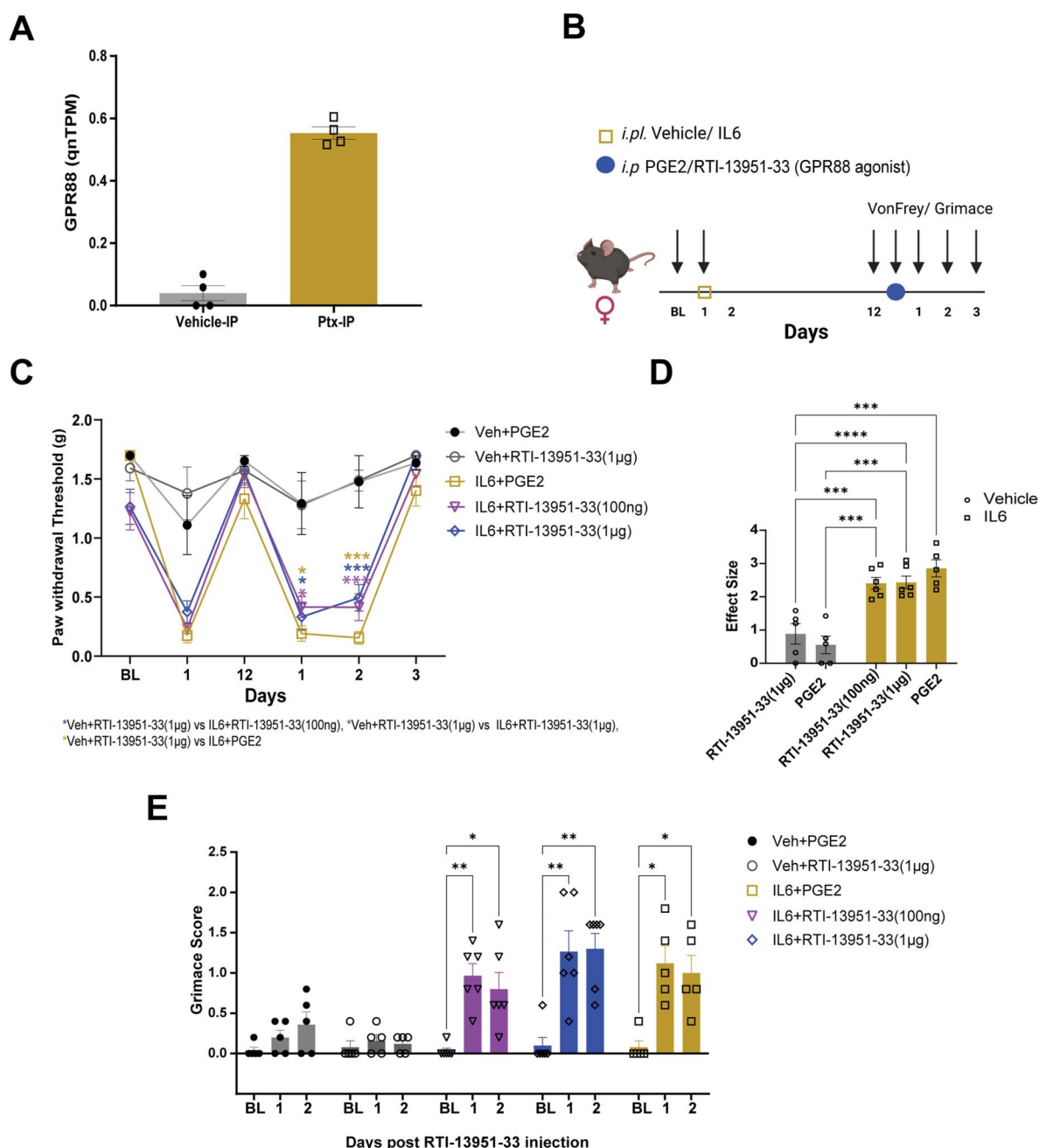


**Figure 4.** GPR88 causes mechanical hypersensitivity in primed animals after interleukin 6 (IL-6) treatment. (A) Expression of *Grp88* mRNA is higher in paclitaxel-treated animals after the resolution of paclitaxel-induced pain behaviors. (B) Schematic representation of dosing paradigm for intraplantar injection of IL-6, prostaglandin E2 (PGE2), or RTI-13951-33 (GPR88 agonist) and von Frey assessment. (C) Hundred-nanogram and 1- $\mu$ g RTI-13951-33 induce mechanical hypersensitivity only in primed mice that were previously treated with IL-6 (2-way analysis of variance [ANOVA],  $F = 5.173$ ,  $P < 0.0001$ ), Tukey multiple comparison test, (vehicle + PGE2,  $N = 5$ , IL-6 + 1  $\mu$ g RTI-13951-33,  $N = 6$ , IL-6 + 100 ng RTI-13951-33,  $N = 6$ , vehicle + 1  $\mu$ g RTI-13951-33,  $N = 5$ ), day 1 post PGE2 or RTI-13951-33, IL-6 + PGE2 vs Veh + 1  $\mu$ g RTI-13951-33,  $P$  value = 0.0205, IL-6 + 1  $\mu$ g RTI-13951-33 vs Veh + 1  $\mu$ g RTI-13951-33,  $P$  value = 0.0311, IL-6 + 100 ng RTI-13951-33 vs Veh + 1  $\mu$ g RTI-13951-33,  $P$  value = 0.0471, day 2 post PGE2 or RTI-13951-33 administration IL-6 + PGE2 vs Veh + 1  $\mu$ g RTI-13951-33,  $P$  value = <0.0001, IL-6 + 1  $\mu$ g RTI-13951-33 vs Veh + 1  $\mu$ g RTI-13951-33,  $P$  value = 0.0005, IL-6 + 100 ng RTI-13951-33 vs Veh + 1  $\mu$ g RTI-13951-33,  $P$  value = 0.0003, Veh + PGE2 vs IL-6 + PGE2,  $P$  value = 0.0153, Veh + PGE2 vs IL-6 + 1  $\mu$ g RTI-13951-33,  $P$  value = 0.0403, Veh + PGE2 vs IL-6 + 100 ng RTI-13951-33,  $P$  value = 0.0287. Data represents mean  $\pm$  SEM. Significance represented as IL-6 + 1  $\mu$ g RTI-13951-33 vs Veh + 1  $\mu$ g RTI-13951-33 (pink\*), IL-6 + 100 ng RTI-13951-33 vs Veh + 1  $\mu$ g RTI-13951-33 (blue\*), Veh + RTI-13951-33 vs IL-6 + PGE2 (yellow\*). (D) Effect size was determined by calculating the sum of the cumulative difference between the value for each time point post-GPR88 agonist administration and the day 12 baseline value. We observed a significant difference for both 100 ng and 1  $\mu$ g RTI-13951-33 treatment between the vehicle group and IL-6 primed animals (2-way ANOVA,  $P$  value = <0.0001), Tukey multiple comparison test, 100 ng RTI-13951-33: IL-6 vs 1  $\mu$ g RTI-13951-33: vehicle,  $P$  value = 0.0002, 100 ng RTI-13951-33: IL-6 vs PGE2: vehicle,  $P$  value = 0.0003, 1  $\mu$ g RTI-13951-33: vehicle vs 1  $\mu$ g RTI-13951-33: IL-6,  $P$  value = <0.0001, 1  $\mu$ g RTI-13951-33: vehicle vs PGE2:IL-6,  $P$  value = 0.0002, 1  $\mu$ g RTI-13951-33:IL-6 vs PGE2: vehicle,  $P$  value = 0.0002, PGE2:vehicle vs PGE2:IL-6,  $P$  value = <0.0001. (E) Grimacing behavior was observed to be significantly different in animals treated with RTI-13951-33 compared with its baseline measurement (2-way ANOVA,  $F = 4.834$ ,  $P$  value = 0.0003, Dunnett multiple comparison test, day 1 IL-6 + PGE2 vs baseline,  $P$  value = 0.0261, IL-6 + 1  $\mu$ g RTI-13951-33 vs baseline,  $P$  value = 0.0051, IL-6 + 100 ng RTI-13951-33 vs baseline,  $P$  value = 0.0022, day 2, IL-6 + PGE2 vs baseline,  $P$  value = 0.0358, IL-6 + 1  $\mu$ g RTI-13951-33 vs baseline,  $P$  value = 0.0024, IL-6 + 100 ng RTI-13951-33 vs baseline,  $P$  value = 0.0282). Data represents mean  $\pm$  SEM. \* $P < 0.05$ ; \*\* $P < 0.01$ ; \*\*\* $P < 0.001$ ; \*\*\*\* $P < 0.0001$ .

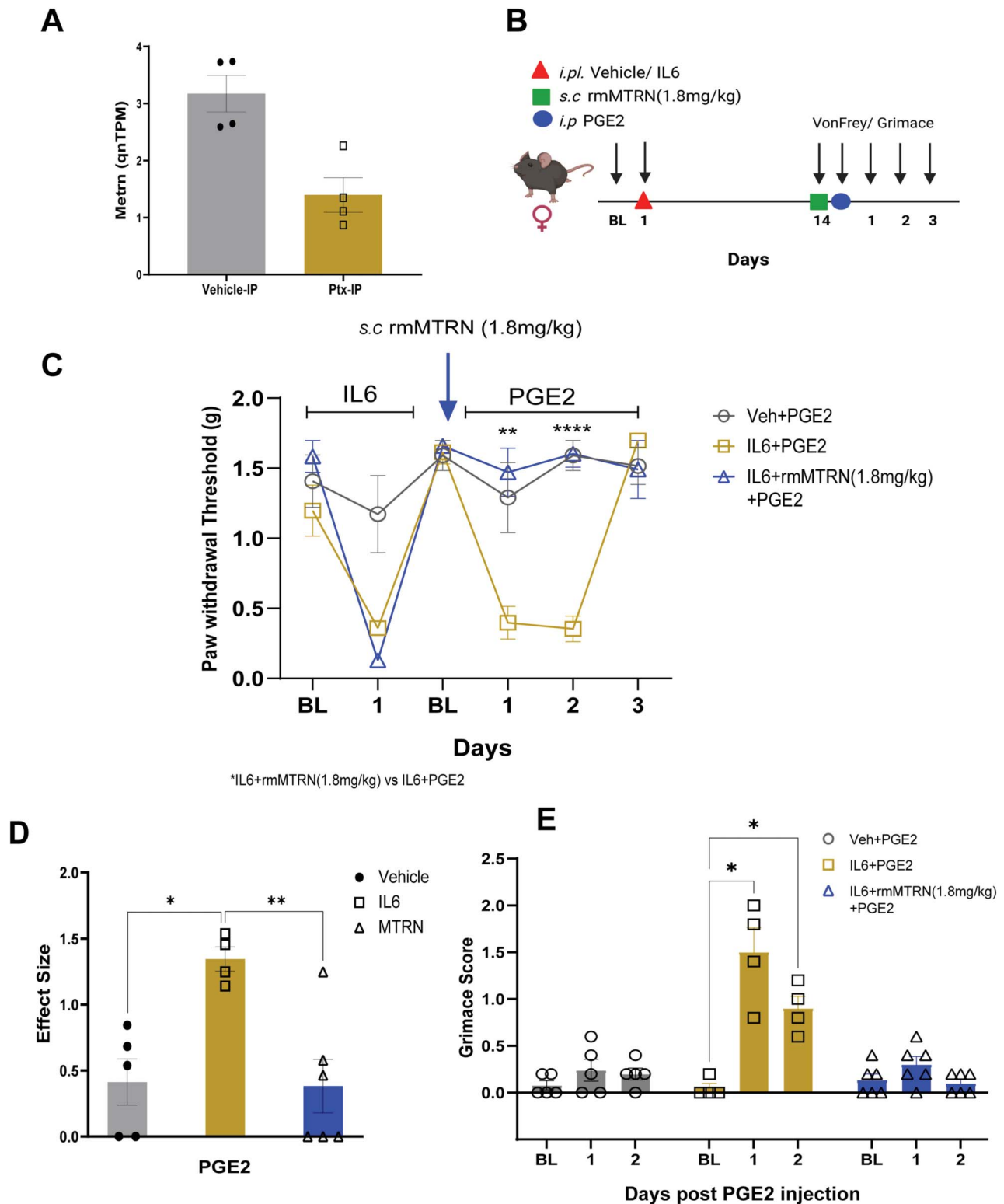


**Figure 5.** Meteorin reverses hyperalgesic priming in animals primed with interleukin 6 (IL-6). (A) Quantile normalized expression of *Metrn* is observed to be decreased in paclitaxel-treated Na,1.8cre/Rosa26<sup>STRAP</sup> mice after the resolution of paclitaxel-induced pain behaviors. (B) Diagram showing the dosing paradigm of IL-6, rmMTRN, and prostaglandin E2 (PGE2) and behavioral testing schedule. (C) 1.8 mg/kg rmMTRN administration an hour before PGE2 injection attenuated the development of mechanical hypersensitivity in IL-6-primed animals (2-way analysis of variance [ANOVA],  $F = 24.77$ ,  $P$  value = <0.0001), Tukey multiple comparison test, day 1 post PGE2 injection, IL-6 + PGE2 vs IL-6 + rmMTRN (1.8 mg/kg) + PGE2,  $P$  value = <0.0023, day 2 post PGE2 injection, IL-6 + PGE2 vs IL-6 + rmMTRN (1.8 mg/kg) + PGE2,  $P$  value = <0.0001, IL-6 + PGE2,  $N = 4$ , Veh + PGE2,  $N = 5$ , IL-6 + rmMTRN (1.8 mg/kg) + PGE2,  $N = 6$ . (D) Effect size was calculated from the first administration of rmMTRN and was observed to be significant between primed animals treated with PGE2 and primed animals administered with rmMTRN and PGE2 (1-way ANOVA, IL-6 + PGE2: IL-6 + rmMTRN [1.8 mg/kg] + PGE2,  $P$  value = <0.0079, IL-6 + PGE2: vehicle + PGE2,  $P$  value = <0.0124). (E) Grimacing behavior was observed to be similar to its baseline measurements in mice administered with rmMTRN (2-way ANOVA,  $F = 10.35$ ,  $P$  value = <0.0001), day 1 post PGE2 injection, IL-6 + PGE2 vs baseline measurement,  $P$  value = 0.0302, day 2, IL-6 + PGE2 vs baseline measurement,  $P$  value = 0.0256, day 1 post PGE2 injection, IL-6 + rmMTRN (1.8 mg/kg) + PGE2 vs baseline measurement of IL-6 + rmMTRN (1.8 mg/kg),  $P$  value = 0.4465, day 2, IL-6 + rmMTRN (1.8 mg/kg) + PGE2 vs baseline measurement of IL-6 + rmMTRN (1.8 mg/kg),  $P$  value = 0.9167. \*  $P < 0.05$ ; \*\*  $P < 0.01$ ; \*\*\*\*  $P < 0.0001$ .



studies that have implicated the receptor in psychiatric disorders.<sup>60</sup> Interestingly, from a pain perspective, GPR88 expression and activation seems to decrease the signaling of coexpressed mu-opioid receptors, including decreased supraspinal analgesia.<sup>25</sup> Whether the receptor can also decrease signaling in peripheral opioid receptors has not been tested but would be of interest for future studies. Although *Gpr88* mRNA is detected in mouse DRG in bulk RNA sequencing studies,<sup>46,58</sup> its expression level is very low and the cell types that express the mRNA are not clear from single nucleus sequencing experiments where it is mostly not detected.<sup>5,50</sup> It is also lowly expressed in human DRG<sup>46,47,57,58</sup> but is detected in a subset of nociceptors that are associated with injury.<sup>57</sup> Based on these findings, it is likely that the *Gpr88* mRNA is normally lowly expressed but its translation efficiency is increased after priming, leading to the increased association with translating ribosomes we detected in our study. The fact that a GPR88 agonist causes mechanical hypersensitivity and grimacing only in primed mice is consistent with this conclusion. This also reveals a new feature of hyperalgesic priming as unprimed mice do not appear to respond at all to a GPR88 agonist. Prostaglandin E2 causes nociceptive responses in unprimed mice with the dose-response shifted dramatically to the left, with lower concentrations causing nociceptive responses, in primed mice.<sup>49</sup>

*Metm* mRNA translation was decreased in primed DRG nociceptors, and systemic administration of Meteorin to mice led to reversal of hyperalgesic priming. Previous studies with Meteorin have suggested that this secreted protein with no known receptor alleviates pain in nerve injury models of neuropathic pain and in the paclitaxel model of chemotherapy-induced neuropathic pain in mice.<sup>23,51,59</sup> This is the first study to demonstrate that Meteorin treatment can block the expression of hyperalgesic priming. Meteorin's biological action has been linked to satellite glial cells and axonal network formation in previous studies, but the source of Meteorin protein has not been determined.<sup>23,42,51,59</sup> *Metm* gene expression is detected in single nucleus RNA sequencing in *Scn10a* expressing cells in the mouse DRG<sup>5,61</sup> and is also detected in these neurons in human DRG.<sup>5,57</sup> Our findings suggest that downregulation of the translation of the *Metm* mRNA in nociceptors likely contributes to the primed state because treatment with Meteorin protein led to a complete and rapid reversal of the expression of hyperalgesic priming. This finding, combined with the previous literature on Meteorin in pain where Meteorin has been shown to disrupt ongoing neuropathic pain.<sup>23,51,59</sup> suggests that Meteorin supplementation may be an effective strategy for pain treatment. Our findings also suggest that Meteorin may play an important role in the transition from acute to chronic pain.

Our study has limitations. First, we focused entirely on female mice. We did this because paclitaxel is mostly used as a chemotherapeutic agent in women and because chronic pain is more prevalent in women.<sup>38</sup> We acknowledge that future studies in male mice are warranted, but we also note that we have and others have already shown efficacy for Meteorin in both male and female animals, suggesting no sex difference for this mediator in the context of pain.<sup>23,51,59</sup> It would also be worth testing whether Meteorin treatment can disrupt the maintenance of priming by giving the Meteorin treatment to primed mice a day or 2 before the expression of priming is tested with PGE2 treatment. Finally, with respect to Meteorin, we hope that these findings will motivate additional efforts to identify the receptor of Meteorin, which will greatly enhance our understanding of this promising therapeutic target. Second, our study focused on a limited number of genes, and a more comprehensive analysis of the entire transcriptome could

uncover additional key players in the maintenance of chronic pain states. From this perspective, our work is a resource that others can use to explore these factors. Finally, we have only focused on nociceptors. It is known that immune cells play an important role in hyperalgesic priming and the promotion and resolution of chronic pain.<sup>10,16,18,24,29,31,32,44</sup> No previous studies have used TRAP sequencing to identify persistent changes in transcriptomes of specific cells after pain has resolved from an initial stimulus. Our work sets a foundation for additional studies in this area of research.

The key takeaway from these experiments is that even after the resolution of overt signs of pain, nociceptors display a reorganization of their translational landscape that contributes to the maintenance of a primed state that makes these neurons susceptible to normally subthreshold stimuli that can now rekindle a state of pain in the organism driven by nociceptor hyperexcitability. These findings have important implications for understanding chronic pain states and for discovery of pain resolution mechanisms that can target the underlying pathology in nociceptors that maintain the susceptibility of the organism to experience pain in response to insults or stimuli that would normally not provoke such a response.

### Conflict of interest statement

G.M. and K.A.P. are employees of Hoba Therapeutics. The remaining authors have no conflicts of interest to declare.

### Acknowledgements

This work was supported by the National Institutes of Health Grant NS065926.

Data availability: RNA sequencing data are available at NCBI GEO database, accession number GSE274093 (<https://www.ncbi.nlm.nih.gov/geo/query/acc.cgi?acc=GSE274093>). All other data are included in the manuscript's figures.

### Supplemental digital content

Supplemental digital content associated with this article can be found online at <http://links.lww.com/PAIN/C210>.

### Article history:

Received 19 August 2024

Received in revised form 30 September 2024

Accepted 8 October 2024

Available online 28 January 2025

### References

- [1] Amorim IS, Kedia S, Kouloulia S, Simbriger K, Gantois I, Jafarnejad SM, Li Y, Kampaite A, Pooters T, Romano N, Gkogkas CG. Loss of eIF4E phosphorylation engenders depression-like behaviors via selective mRNA translation. *J Neurosci* 2018;38:2118–33.
- [2] Andratsch M, Mair N, Constantin CE, Scherbakov N, Benetti C, Quarta S, Vogl C, Sailer CA, Uceyler N, Brockhaus J, Martini R, Sommer C, Zeilhofer HU, Muller W, Kuner R, Davis JB, Rose-John S, Kress M. A key role for gp130 expressed on peripheral sensory nerves in pathological pain. *J Neurosci* 2009;29:13473–83.
- [3] Araldi D, Ferrari LF, Levine JD. Repeated mu-opioid exposure induces a novel form of the hyperalgesic priming model for transition to chronic pain. *J Neurosci* 2015;35:12502–17.
- [4] Barragan-Iglesias P, Lou TF, Bhat VD, Megat S, Burton MD, Price TJ, Campbell ZT. Inhibition of Poly(A)-binding protein with a synthetic RNA mimic reduces pain sensitization in mice. *Nat Commun* 2018;9:10.
- [5] Bhuiyan SA, Xu M, Yang L, Semizoglou E, Bhatia P, Pantaleo KI, Tochitsky I, Jain A, Erdogan B, Blair S, Cat V, Mwirigi JM,

- Sankaranarayanan I, Tavares-Ferreira D, Green U, McIvried LA, Copits BA, Bertels Z, Del Rosario JS, Widman AJ, Slivicki RA, Yi J, Sharif-Naeini R, Woolf CJ, Lennerz JK, Whited JL, Price TJ, Renthal W. Harmonized cross-species cell atlases of trigeminal and dorsal root ganglia. *Sci Adv* 2024;10:ead9173.
- [6] Bogen O, Alessandri-Haber N, Chu C, Gear RW, Levine JD. Generation of a pain memory in the primary afferent nociceptor triggered by PKC $\alpha$  activation of CPEB. *J Neurosci* 2012;32:2018–26.
- [7] Chaplan SR, Bach FW, Pogrel JW, Chung JM, Yaksh TL. Quantitative assessment of tactile allodynia in the rat paw. *J Neurosci Methods* 1994; 53:55–63.
- [8] David ET, Yousuf MS, Mei HR, Jain A, Krishnagiri S, Elahi H, Venkatesan R, Srikanth KD, Dussor G, Dalva MB, Price TJ. ephrin-B2 promotes nociceptive plasticity and hyperalgesic priming through EphB2-MNK-elf4E signaling in both mice and humans. *Pharmacol Res* 2024;206: 107284.
- [9] Dina OA, Green PG, Levine JD. Role of interleukin-6 in chronic muscle hyperalgesic priming. *Neuroscience* 2008;152:521–5.
- [10] Eijkelkamp N, Steen-Louws C, Hartgring SA, Willemen HL, Prado J, Lafeber FP, Heijnen CJ, Hack CE, van Roon JA, Kavelaars A. IL4-10 fusion protein is a novel drug to treat persistent inflammatory pain. *J Neurosci* 2016;36:7353–63.
- [11] Ferrari LF, Araldi D, Levine JD. Distinct terminal and cell body mechanisms in the nociceptor mediate hyperalgesic priming. *J Neurosci* 2015;35:6107–16.
- [12] Ferrari LF, Bogen O, Chu C, Levine JD. Peripheral administration of translation inhibitors reverses increased hyperalgesia in a model of chronic pain in the rat. *J Pain* 2013;14:731–8.
- [13] Ferrari LF, Bogen O, Levine JD. Role of nociceptor  $\alpha$ CaMKII in transition from acute to chronic pain (hyperalgesic priming) in male and female rats. *J Neurosci* 2013;33:11002–11.
- [14] Ferrari LF, Bogen O, Reichling DB, Levine JD. Accounting for the delay in the transition from acute to chronic pain: axonal and nuclear mechanisms. *J Neurosci* 2015;35:495–507.
- [15] Garza Carbajal A, Ebersberger A, Thiel A, Ferrari L, Acuna J, Brosig S, Isensee J, Moeller K, Siobal M, Rose-John S, Levine J, Schaible HG, Hucho T. Oncostatin M induces hyperalgesic priming and amplifies signaling of cAMP to ERK by RapGEF2 and PKA. *J Neurochem* 2021;157:1821–37.
- [16] Ghazisaeidi S, Muley MM, Salter MW. Neuropathic pain: mechanisms, sex differences, and potential therapies for a global problem. *Annu Rev Pharmacol Toxicol* 2023;63:565–83.
- [17] Gkogkas CG, Khoutorsky A, Cao R, Jafarnejad SM, Prager-Khoutorsky M, Giannakas N, Kaminari A, Fragkouli A, Nader K, Price TJ, Konicek BW, Graff JR, Tzinia AK, Lacaille JC, Sonenberg N. Pharmacogenetic inhibition of elf4E-dependent Mmp9 mRNA translation reverses fragile X syndrome-like phenotypes. *Cell Rep* 2014;9:1742–55.
- [18] Gregus AM, Levine IS, Eddinger KA, Yaksh TL, Buczynski MW. Sex differences in neuroimmune and glial mechanisms of pain. *PAIN* 2021; 162:2186–200.
- [19] Heiman M, Kulicke R, Fenster RJ, Greengard P, Heintz N. Cell type-specific mRNA purification by translating ribosome affinity purification (TRAP). *Nat Protoc* 2014;9:1282–91.
- [20] Heiman M, Schaefer A, Gong S, Peterson JD, Day M, Ramsey KE, Suarez-Farinas M, Schwarz C, Stephan DA, Surmeier DJ, Greengard P, Heintz N. A translational profiling approach for the molecular characterization of CNS cell types. *Cell* 2008;135:738–48.
- [21] Inyang KE, McDougal TA, Ramirez ED, Williams M, Laumet G, Kavelaars A, Heijnen CJ, Burton M, Dussor G, Price TJ. Alleviation of paclitaxel-induced mechanical hypersensitivity and hyperalgesic priming with AMPK activators in male and female mice. *Neurobiol Pain* 2019;6: 100037.
- [22] Ji RR, Xu ZZ, Strichartz G, Serhan CN. Emerging roles of resolvins in the resolution of inflammation and pain. *Trends Neurosci* 2011;34:599–609.
- [23] Jorgensen JR, Xu XJ, Arnold HM, Munro G, Hao JX, Pepinsky B, Huang C, Gong BJ, Wiesenfeld-Hallin Z, Wahlberg LU, Johansen TE. Meteorin reverses hypersensitivity in rat models of neuropathic pain. *Exp Neurol* 2012;237:260–6.
- [24] Kavelaars A, Heijnen CJ. T cells as guardians of pain resolution. *Trends Mol Med* 2021;27:302–13.
- [25] Laboute T, Gandia J, Pellissier LP, Corde Y, Rebeillard F, Gallo M, Gauthier C, Leaute A, Diaz J, Poupon A, Kieffer BL, Le Merrer J, Becker JA. The orphan receptor GPR88 blunts the signaling of opioid receptors and multiple striatal GPCRs. *Elife* 2020;9:e50519.
- [26] Lackovic J, Price TJ, Dussor G. De novo protein synthesis is necessary for priming in preclinical models of migraine. *Cephalalgia* 2021;41:237–46.
- [27] Lackovic J, Price TJ, Dussor G. MNK1/2 contributes to periorbital hypersensitivity and hyperalgesic priming in preclinical migraine models. *Brain* 2023;146:448–54.
- [28] Langford DJ, Bailey AL, Chanda ML, Clarke SE, Drummond TE, Echols S, Glick S, Ingrao J, Klassen-Ross T, Lacroix-Fralish ML, Matsumiya L, Sorge RE, Sotocinal SG, Tabaka JM, Wong D, van den Maagdenberg AM, Ferrari MD, Craig KD, Mogil JS. Coding of facial expressions of pain in the laboratory mouse. *Nat Methods* 2010;7:447–9.
- [29] Laumet G, Bavencoffe A, Edralin JD, Huo XJ, Walters ET, Dantzer R, Heijnen CJ, Kavelaars A. Interleukin-10 resolves pain hypersensitivity induced by cisplatin by reversing sensory neuron hyperexcitability. *PAIN* 2020;161:2344–52.
- [30] Liu L, Zhu Y, Noe M, Li Q, Pasricha PJ. Neuronal transforming growth factor beta signaling via SMAD3 contributes to pain in animal models of chronic pancreatitis. *Gastroenterology* 2018;154:2252–65.e2.
- [31] Makker PG, Duffy SS, Lees JG, Perera CJ, Tonkin RS, Butovsky O, Park SB, Goldstein D, Moalem-Taylor G. Characterisation of immune and neuroinflammatory changes associated with chemotherapy-induced peripheral neuropathy. *PLoS One* 2017;12:e0170814.
- [32] Mecklenburg J, Wangzhou A, Hovhannisyan AH, Barba-Escobedo P, Shein SA, Zou Y, Weldon K, Lai Z, Goffin V, Dussor G, Tumanov AV, Price TJ, Akopian AN. Sex-dependent pain trajectories induced by prolactin require an inflammatory response for pain resolution. *Brain Behav Immun* 2022;101:246–63.
- [33] Megat S, Ray PR, Moy JK, Lou TF, Barragan-Iglesias P, Li Y, Pradhan G, Wangzhou A, Ahmad A, Burton MD, North RY, Dougherty PM, Khoutorsky A, Sonenberg N, Webster KR, Dussor G, Campbell ZT, Price TJ. Nociceptor translational profiling reveals the regulator-rag GTPase complex as a critical generator of neuropathic pain. *J Neurosci* 2019;39:393–411.
- [34] Megat S, Ray PR, Tavares-Ferreira D, Moy JK, Sankaranarayanan I, Wangzhou A, Fang Lou T, Barragan-Iglesias P, Campbell ZT, Dussor G, Price TJ. Differences between dorsal root and trigeminal ganglion nociceptors in mice revealed by translational profiling. *J Neurosci* 2019; 39:6829–47.
- [35] Melemedjian OK, Asiedu MN, Tillu DV, Peebles KA, Yan J, Ertz N, Dussor GO, Price TJ. IL-6- and NGF-induced rapid control of protein synthesis and nociceptive plasticity via convergent signaling to the elf4F complex. *J Neurosci* 2010;30:15113–23.
- [36] Melemedjian OK, Tillu DV, Moy JK, Asiedu MN, Mandell EK, Ghosh S, Dussor G, Price TJ. Local translation and retrograde axonal transport of CREB regulates IL-6-induced nociceptive plasticity. *Mol Pain* 2014;10: 45.
- [37] Mitchell ME, Torrijos G, Cook LF, Mwirigi JM, He L, Shiers S, Price TJ. Interleukin-6 induces nascent protein synthesis in human dorsal root ganglion nociceptors primarily via MNK-elf4E signaling. *Neurobiol Pain* 2024;16:100159.
- [38] Mogil JS, Parisien M, Esfahani SJ, Diatchenko L. Sex differences in mechanisms of pain hypersensitivity. *Neurosci Biobehav Rev* 2024;163: 105749.
- [39] Moriyama T, Higashi T, Togashi K, Iida T, Segi E, Sugimoto Y, Tominaga T, Narumiya S, Tominaga M. Sensitization of TRPV1 by EP1 and IP reveals peripheral nociceptive mechanism of prostaglandins. *Mol Pain* 2005;1:3.
- [40] Moy JK, Khoutorsky A, Asiedu MN, Black BJ, Kuhn JL, Barragan-Iglesias P, Megat S, Burton MD, Burgos-Vega CC, Melemedjian OK, Boitano S, Vagner J, Gkogkas CG, Pancrazio JJ, Mogil JS, Dussor G, Sonenberg N, Price TJ. The MNK-elf4E signaling Axis contributes to injury-induced nociceptive plasticity and the development of chronic pain. *J Neurosci* 2017;37:7481–99.
- [41] Moy JK, Khoutorsky A, Asiedu MN, Dussor G, Price TJ. elf4E phosphorylation influences bdnf mRNA translation in mouse dorsal root ganglion neurons. *Front Cell Neurosci* 2018;12:29.
- [42] Nishino J, Yamashita K, Hashiguchi H, Fujii H, Shimazaki T, Hamada H. Meteorin: a secreted protein that regulates glial cell differentiation and promotes axonal extension. *EMBO J* 2004;23:1998–2008.
- [43] Obreja O, Schmelz M, Poole S, Kress M. Interleukin-6 in combination with its soluble IL-6 receptor sensitises rat skin nociceptors to heat, in vivo. *PAIN* 2002;96:57–62.
- [44] Parisien M, Lima LV, Dagostino C, El-Hachem N, Drury GL, Grant AV, Huising J, Verma V, Meloto CB, Silva JR, Dutra GGS, Markova T, Dang H, Tessier PA, Slade GD, Nackley AG, Ghasemlou N, Mogil JS, Allegri M, Diatchenko L. Acute inflammatory response via neutrophil activation protects against the development of chronic pain. *Sci Transl Med* 2022; 14:eab9954.
- [45] Price TJ, Inyang KE. Commonalities between pain and memory mechanisms and their meaning for understanding chronic pain. *Prog Mol Biol Transl Sci* 2015;131:409–34.
- [46] Ray P, Torck A, Quigley L, Wangzhou A, Neiman M, Rao C, Lam T, Kim JY, Kim TH, Zhang MQ, Dussor G, Price TJ. Comparative transcriptome profiling of the human and mouse dorsal root ganglia: an RNA-seq-based

- resource for pain and sensory neuroscience research. *PAIN* 2018;159:1325–45.
- [47] Ray PR, Shiers S, Caruso JP, Tavares-Ferreira D, Sankaranarayanan I, Uhelski ML, Li Y, North RY, Tatsui C, Dussor G, Burton MD, Dougherty PM, Price TJ. RNA profiling of human dorsal root ganglia reveals sex differences in mechanisms promoting neuropathic pain. *Brain* 2023;146:749–66.
- [48] Reichling DB, Green PG, Levine JD. The fundamental unit of pain is the cell. *PAIN* 2013;154(suppl 1):S2–9.
- [49] Reichling DB, Levine JD. Critical role of nociceptor plasticity in chronic pain. *Trends Neurosci* 2009;32:611–8.
- [50] Renthal W, Tochitsky I, Yang L, Cheng YC, Li E, Kawaguchi R, Geschwind DH, Woolf CJ. Transcriptional reprogramming of distinct peripheral sensory neuron subtypes after axonal injury. *Neuron* 2020;108:128–44.e9.
- [51] Sankaranarayanan I, Tavares-Ferreira D, He L, Kume M, Mwirigi JM, Madsen TM, Petersen KA, Munro G, Price TJ. Meteorin alleviates paclitaxel-induced peripheral neuropathic pain in mice. *J Pain* 2023;24:555–67.
- [52] Sankaranarayanan I, Tavares-Ferreira D, Mwirigi JM, Mejia GL, Burton MD, Price TJ. Inducible co-stimulatory molecule (ICOS) alleviates paclitaxel-induced neuropathic pain via an IL-10-mediated mechanism in female mice. *J Neuroinflammation* 2023;20:32.
- [53] St-Jacques B, Ma W. Peripheral prostaglandin E2 prolongs the sensitization of nociceptive dorsal root ganglion neurons possibly by facilitating the synthesis and anterograde axonal trafficking of EP4 receptors. *Exp Neurol* 2014;261:354–66.
- [54] Stirling LC, Forlani G, Baker MD, Wood JN, Matthews EA, Dickenson AH, Nassar MA. Nociceptor-specific gene deletion using heterozygous Nav1.8-Cre recombinase mice. *PAIN* 2005;113:27–36.
- [55] Stock JL, Shinjo K, Burkhardt J, Roach M, Taniguchi K, Ishikawa T, Kim HS, Flannery PJ, Coffman TM, McNeish JD, Audoly LP. The prostaglandin E2 EP1 receptor mediates pain perception and regulates blood pressure. *J Clin Invest* 2001;107:325–31.
- [56] Tavares-Ferreira D, Ray PR, Sankaranarayanan I, Mejia GL, Wangzhou A, Shiers S, Uttarkar R, Megat S, Barragan-Iglesias P, Dussor G, Akopian AN, Price TJ. Sex differences in nociceptor transcriptomes contribute to divergent prostaglandin signaling in male and female mice. *Biol Psychiatry* 2022;91:129–40.
- [57] Tavares-Ferreira D, Shiers S, Ray PR, Wangzhou A, Jeevakumar V, Sankaranarayanan I, Cervantes AM, Reese JC, Chamezian A, Copits BA, Dougherty PM, Gereau RW IV, Burton MD, Dussor G, Price TJ. Spatial transcriptomics of dorsal root ganglia identifies molecular signatures of human nociceptors. *Sci Transl Med* 2022;14:eabj8186.
- [58] Wangzhou A, McIlvried LA, Paige C, Barragan-Iglesias P, Shiers S, Ahmad A, Guzman CA, Dussor G, Ray PR, Gereau RW IV, Price TJ. Pharmacological target-focused transcriptomic analysis of native vs cultured human and mouse dorsal root ganglia. *PAIN* 2020;161:1497–517.
- [59] Xie JY, Qu C, Munro G, Petersen KA, Porreca F. Antihyperalgesic effects of Meteorin in the rat chronic constriction injury model: a replication study. *PAIN* 2019;160:1847–55.
- [60] Ye N, Li B, Mao Q, Wold EA, Tian S, Allen JA, Zhou J. Orphan receptor GPR88 as an emerging neurotherapeutic target. *ACS Chem Neurosci* 2019;10:190–200.
- [61] Zeisel A, Hochgerner H, Lonnerberg P, Johnsson A, Memic F, van der Zwan J, Haring M, Braun E, Borm LE, La Manno G, Codeluppi S, Furlan A, Lee K, Skene N, Harris KD, Hjerling-Leffler J, Arenas E, Ernfors P, Marklund U, Linnarsson S. Molecular architecture of the mouse nervous system. *Cell* 2018;174:999–1014.e22.
- [62] Zhang XD. Illustration of SSMD, z score, SSMD\*, z\* score, and t statistic for hit selection in RNAi high-throughput screens. *J Biomol Screen* 2011;16:775–85.
- [63] Zhang XD, Lacson R, Yang R, Marine SD, McCampbell A, Toolan DM, Hare TR, Kajdas J, Berger JP, Holder DJ, Heyse JF, Ferrer M. The use of SSMD-based false discovery and false nondiscovery rates in genome-scale RNAi screens. *J Biomol Screen* 2010;15:1123–31.
- [64] Zhu Y, Colak T, Shenoy M, Liu L, Mehta K, Pai R, Zou B, Xie XS, Pasricha PJ. Transforming growth factor beta induces sensory neuronal hyperexcitability, and contributes to pancreatic pain and hyperalgesia in rats with chronic pancreatitis. *Mol Pain* 2012;8:65.